Respiratory Motion-Compensated Radial DCE-MRI of Chest and Abdominal Lesions

W. Lin[1], J. Guo[1], M. A. Rosen[1], and H. K. Song[1]

[1]Department of Radiology, University of Pennsylvania, Philadelphia, PA, United States

Introduction

Dynamic contrast-enhanced MRI (DCE-MRI) has emerged as a prime method for evaluating tumor vascularity and in assessing the effectiveness of new antiangiogenic and antivascular agents. DCE-MRI of lesions located in the chest and the abdomen, common areas for tumor metastases, however, is often hindered by respiratory motion. Lesion displacement and blurring make measurements difficult, and precludes accurate pixel-by-pixel analysis. The purpose of this work is to develop a robust 3D DCE-MRI technique based on the golden-angle radial acquisition scheme (1), which allows for both effective motion compensation via retrospective self-gating (2) and high temporal resolution for accurate pixel-based perfusion analysis of lesions located in the lung and liver.

Methods

The proposed radial DCE-MRI technique is summarized in **Fig. 1**. A 3D golden-angle hybrid radial acquisition scheme was modified from a conventional spoiled gradient echo sequence. The inner slice-encoding loop is phase encoded, while the two in-plane axes utilize a golden-angle radial acquisition scheme (1), in which a fixed angular offset of $\theta \approx 111.25^0$ advances successive view angles. Following the free-breathing data acquisition, the peak signal of views at $k_z = 0$ (acquired every N*TR, where N is number of slice encodings) is processed to generate a respiratory self-gating signal (**Fig. 2**). Following a high-pass filter to isolate signal variations due to respiration from those due to contrast enhancement, the end-expiratory peaks are detected, and consecutive views (34-55 views depending on the respiratory rate) within each respiratory cycle grouped into individual segments for subsequent reconstruction.

End-expiratory segments are used in this work, since they exhibit the least amount of both intra-segment (during a single respiratory cycle) and inter-segment (between different respiratory periods) motion. To further compensate for any residual intra-segment lesion motion, a regional radial autofocusing method was developed, assuming motion is limited to 3D translations, by optimizing image entropy (3) using a 5th order polynomial motion model. For inter-segment motion, the relative lesion displacements among different respiratory cycles are detected from the maximal 3D image correlation computed over the lesion ROI, and the images are subsequently aligned.

Since each motion-compensated end-expiratory segments consists of only 34-55 views (while each readout line has 192 points), significant streaks will appear and image SNR is relatively low. There are two ways to reduce these artifacts: k-space weighted image contrast (KWIC) radial filtering method (4) and principal component analysis (PCA) (5). In KWIC processing, for each image, data from only one segment is used in the central k-space region, while increasing number of segments encode the outer regions, all the while satisfying the Nyquist criterion. In PCA, the entire undersampled dynamic series is statistically analyzed, separating them into an orthogonal set of temporal response functions and their corresponding images (weighting functions). Components contributing primarily to streaks and noise are then removed to enhance image quality.

Since respiratory motion in the aorta is minimal, the arterial input function (AIF) can be sampled without respiratory gating using a sliding window reconstruction (34 views per image), permitting an AIF sampling period of 1.4 sec. For baseline T_1 measurement, a dual flip-angle, free-breathing radial technique described previously (6) is carried out prior to the DCE-MRI.

In vivo examinations were performed utilizing the proposed strategy: one patient with a metastatic lung lesion, and a second with a tumor in the liver. The patients were imaged in a double injection protocol, where the proposed technique followed a standard Cartesian DCE-MRI exam. A pixel-by-pixel perfusion model fitting was performed on the lesions using a two-compartment model (7) to determine volume transfer coefficient K^{trans} and extracellular extravascular volume fraction v_e.

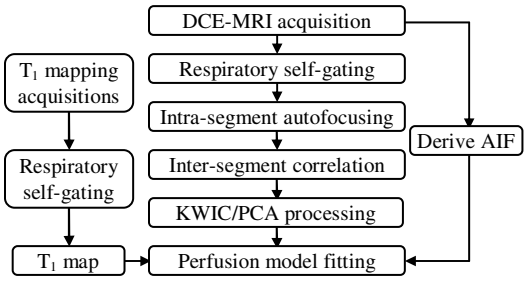

Fig. 1 Proposed respiratory motion-compensated radial DCE-MRI method.

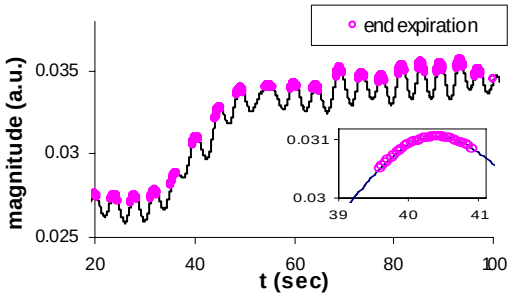

Fig. 2 Respiratory self-gating signal from a radial DCE-MRI acquisition. Inset is a zoomed plot of one respiratory cycle.

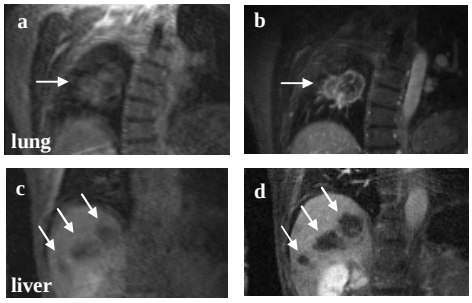

Fig. 3 Post-contrast images acquired using a Cartesian acquisition (a, c) and the proposed radial technique with PCA (b) and KWIC (d) processing. Lesions are indicated by arrows.

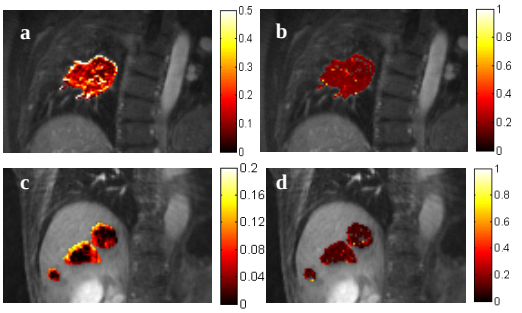

Fig. 4 K^{trans} (1/min) (a, c) and v_e (b, d) maps.

Results and Discussions

Figure 3 compares the images from the standard Cartesian and the proposed radial DCE-MRI methods for the two patients, clearly demonstrating the effectiveness of our strategy. The self-gating procedure removed most of the image blurring, while inter- and intra-segment motion compensation further sharpened the lesion boundaries. Furthermore, KWIC and PCA processing effectively removed the streaking artifacts and enhanced SNR. Both KWIC and PCA yield similar image quality. Root mean square fitting errors of the lung lesion pixels to the model was reduced by 61% and 74% after KWIC and PCA, respectively. **Figure 4** shows the resulting K^{trans} and v_e maps. Such high resolution perfusion parameter maps are not possible with conventional Cartesian techniques due to respiratory motion. In summary, our proposed technique incorporates respiratory self-gating, autofocusing and image registration to effectively compensate for respiratory motion, and utilizes KWIC and PCA to further enhance the image quality of the dynamic series. The feasibility to acquire accurate pixel-wise perfusion parameter maps of chest and abdominal lesions is demonstrated in patient studies.

Acknowledgements: Siemens Medical Solutions.

References

[1] Winkelmann S, et al. *IEEE Tran Med Imaging* 2007; 68-76. [2] Larson AC, et al. *Magn Reson Med* 2004; 51: 93-102. [3] Atkinson D, et al. *IEEE Tran Med Imaging* 1997; 16(6):903-910. [4] Song HK, et al. *Magn Reson Med* 2004; 52: 815-824. [5] Martel AL, et al. *Proc. ISMRM*. 2005;1861. [6] Lin W, et al. *Proc. ISMRM*. 2007; 1791. [7] Tofts PS, et al. *Magn Reson Med* 1991;17:357-367.